



HAL
open science

Mechanical and thermal modification of mordenite-rich tuff and its effect on cement pastes

Meriem Meziani, Nordine Leklou, Nasser Chelouah, Ouali Amiri

► To cite this version:

Meriem Meziani, Nordine Leklou, Nasser Chelouah, Ouali Amiri. Mechanical and thermal modification of mordenite-rich tuff and its effect on cement pastes. *Construction and Building Materials*, 2022, 318, pp.126008. 10.1016/j.conbuildmat.2021.126008 . hal-04731239

HAL Id: hal-04731239

<https://hal.science/hal-04731239v1>

Submitted on 10 Oct 2024

HAL is a multi-disciplinary open access archive for the deposit and dissemination of scientific research documents, whether they are published or not. The documents may come from teaching and research institutions in France or abroad, or from public or private research centers.

L'archive ouverte pluridisciplinaire **HAL**, est destinée au dépôt et à la diffusion de documents scientifiques de niveau recherche, publiés ou non, émanant des établissements d'enseignement et de recherche français ou étrangers, des laboratoires publics ou privés.



Distributed under a Creative Commons Attribution 4.0 International License

Mechanical and thermal modification of mordenite-rich tuff and its effect on cement pastes

Meriem Meziani¹, Nordine Leklou², Nasser Chelouah¹, Ouali Amiri²

¹Laboratoire de Génie de la Construction et d'architecture, Faculté de Technologie, Université de Bejaia,
06000 Bejaia, Algérie

meriem.meziani@univ-bejaia.dz , nasser_chelouah@yahoo.fr

²Université de Nantes, IUT de Saint-Nazaire, GeM UMR-CNRS 6183, 58 rue Michel Ange, BP 420-
44600 Saint-Nazaire, France

nordine.leklou@univ-nantes.fr , ouali.amiri@univ-nantes.fr

Abstract

To overcome performance deficiencies of the raw mordenite-rich tuff in the partial replacement of Portland cement in cement paste, the material was subjected to different treatments: calcination at 300 °C and 500 °C, grinding to very high specific surface areas, co-grinding with Portland cement, and separate or co-grinding with granulate blast furnace slag. The resulting materials were examined by tracking changes in density, particle shapes, and size distributions. The blended cement pastes were examined by monitoring the water demand, setting time, hydration process by isothermal microcalorimetry, degree of hydration, non-evaporable water content and free Ca(OH)₂ by TGA-DSC analysis. The findings provide clear evidence that with the activation techniques, the performance of the raw mordenite-rich tuff is improved.

Keywords: mordenite-rich tuff, treatment techniques, calcination, grinding

1. Introduction

1 Many natural materials are currently used as pozzolanic agents aimed at improving the quality of
2 cement-based materials. Natural zeolites are among the most common and promising minerals
3 for many civil, environmental, and chemical applications. Despite their distinct crystalline
4 structure, their pozzolanic activity is almost as high as that of amorphous mineral additives [1].
5 Therefore, they could be used as an alternative to artificial pozzolanic material to replace parts of
6 Portland cement. Their use as natural pozzolans has increased markedly [1,2] because of their
7 abundance, low extraction and processing costs, large and diverse deposits, low environmental
8 impact, and remarkable physical and chemical properties [3]. Despite these obvious advantages,
9 the properties of zeolites vary greatly between species [4]. Mordenite, heulandite, and
10 clinoptilolite are the most common natural zeolites on earth; the last two have the same
11 crystalline structure and are the most widely used as natural pozzolans, while mordenite is used
12 in smaller quantities [5,6]. In addition, there is limited information about the properties and
13 hydration characteristics of blended cements incorporating mordenite. Some studies have looked
14 into the use of mordenite as a supplementary cementitious material (SCM) to see how it
15 performs in cement-based systems and its pozzolanic behaviour. It was revealed that mortars
16 made with partial replacement of cement with mordenite showed a delay in initial and final
17 setting times, greater consistency, lower fluidity, and lower density [7]. The pozzolanic reaction
18 between mordenite zeolite and the hydration products of cement is enhanced by the mordenite
19 content in the samples and depends on the Si/Al ratio and the surface area [8]. Other researchers
20 found that tuffs rich in mordenite must be calcined at 760 for 12 h to achieve optimal
21 pozzolanicity [9]. The pozzolanic activity of natural mordenite-type zeolite was determined
22 during a reaction with a saturated lime solution at 40 °C. However, the pozzolanic reaction is not
23 responsible for all the Ca²⁺ consumed in solution; zeolite transformation from mordenite to
24 clinoptilolite has been observed [10]. Higher specific surface areas yield higher short-term
25

26 pozzolanic activity when portlandite is consumed by mixing lime with mordenite tuffs ground to
27 different grain sizes [11].

28 Willing to contribute to a state of the art knowledge about the basic mechanisms related to
29 mordenite-rich tuff effects on cementitious materials, we have investigated, in a previous
30 research [12], the benefits of its use as a partial replacement (up to 20%) of Portland cement,
31 from the physico—mechanical and microstructural point of view. The first stage of this study
32 focused on the pastes, including water requirement, setting time, hydration heat and free
33 Ca(OH)_2 content.

34 It was found that mixtures containing mordenite-rich tuff had the potential to replace Portland
35 cement by up to 20%. Incorporation of the mordenite-rich tuff increased the hydration heat up to
36 7 h and accelerated the appearance of the maximum thermal effect by allowing the C_3A to
37 undergo renewed rapid hydration and convert the ettringite to monosulfoaluminate. The water
38 demand of mordenite-rich tuff-blended cement pastes rose as the tuff content increased due to
39 the micropores inherent in its structure. The addition of the mordenite-rich tuff slowed the initial
40 setting time while speeding up the final setting time. The free Ca(OH)_2 levels in cement pastes
41 containing up to 20% mordenite-rich tuff are 7.5%, 9%, and 21% lower than in control paste at
42 7, 28, and 90 days, respectively. Because portlandite is a reactive compound that can cause
43 durability issues, the measured free Ca(OH)_2 content in the blended cement pastes must be
44 further reduced. As a result, the reactivity of mordenite-rich tuff with lime was termed
45 insufficient. The use of mordenite-rich tuff in its natural state is not always as effective as it
46 could be. Then, the improvement of its reactivity could possibly overcome this shortcoming.
47 According to the researchers, the most successful treatments are calcination, milling, and
48 chemical activation [13–16].

49 Research has been done to improve pozzolanic activity by subjecting the natural zeolite to
50 calcination or milling pre-treatments [17–19]. However, little is known about the mechanical and
51 thermal activations of mordenite-rich tuff and their impact on cement-based material properties
52 [20].

53 Milling reduces particle size distributions, increasing specific surface area and reaction speed,
54 but the crystalline structure of natural zeolite is unaffected. Three approaches were used to
55 extend the limits of conventional milling: milling the material to very high specific surface areas
56 to make it as reactive as possible; separate or co-grinding the material with GGBFS; as well as
57 its co-grinding with Portland cement.

58 A calcination pre-treatment alternative has been used to increase mordenite-rich tuff pozzolanic
59 activity.. The objective of the calcination pre-treatment was to improve the physical properties
60 and break the crystalline structure of the material to allow it to react faster or more efficiently as
61 a pozzolan, resulting in an improved performance in cementitious systems.

62 The purpose of this study was to assess the behaviour of mordenite-rich tuff as a supplementary
63 cementitious material as well as the performance of this raw natural pozzolan versus pre-treated
64 mordenite-rich tuff by calcination or milling, with substitution percentages of 5–10–15–20% in
65 ordinary Portland cement. Variable milling parameters and calcination temperatures are used to
66 achieve this. The treated tuffs were compared to the raw mordenite-rich tuff in terms of density,
67 specific surface area, particle size and shape, water requirement, setting time, hydration process,
68 Ca(OH)_2 content, non-evaporable water content, and degree of hydration to show how the
69 activation techniques perform on the tuff powder and pastes.

70 Experimental techniques including isothermal microcalorimetry, thermogravimetric (TGA)
71 coupled with differential scanning calorimetry (DSC), and scanning electron microscopy (SEM)
72 were implemented. Using these techniques yielded new information on the effects of raw and
73 pre-treated mordenite-rich tuff on PC hydration and Ca(OH)_2 consumption, as well as a better
74 understanding of the fresh and hardened performance of the paste samples.

75

2. Presentation of activation techniques

2.1. Thermal activation

In the thermal treatment by calcination, the heating time and the type of cooling are the parameters of great importance in the activation of a pozzolan. The optimum calcination temperature corresponds to the temperature at which the pozzolan minerals crystallize without being followed by recrystallization. The stability of the crystal plays an essential role in the solubility. This is the reason why, in a metastable state, calcined pozzolans are more reactive than in a natural, more stable state [21]. In addition, cooling has a great influence on the stability of minerals; to reach better reactivity, the cooling must be rapid enough to freeze the minerals in their metastable states acquired at the optimum calcination temperature. Notwithstanding the importance of these parameters, the literature does not record any standard calcination test setting other than the heating and cooling methods.

Calcination procedure

The raw mordenite-rich tuff powder defined in the previous research [12] was calcined in a Nabertherm type P330 programmer furnace at 300 °C or 500 °C. In porcelain crucibles measuring 6 cm in high and 4 cm in diameter, 30 grams of tuff were heated at a heating rate of 10 °C/min to reach the desired temperature; this temperature was then kept constant for 5 hours. At the end of this period, the calcined tuffs were quickly transferred into a desiccator and cooled at ambient temperature (20 °C).

2.2. Mechanical activation

Using the pozzolan reactivity's improvement method, mechanical activation, traditionally achieved by grinding grains to a higher specific surface area, proved to be an easy, practical, and efficient technique.

The objective of this technique is to improve the properties of mordenite-rich tuff in order to enhance its ability to react faster or more efficiently. This will result in better performance in cement systems.

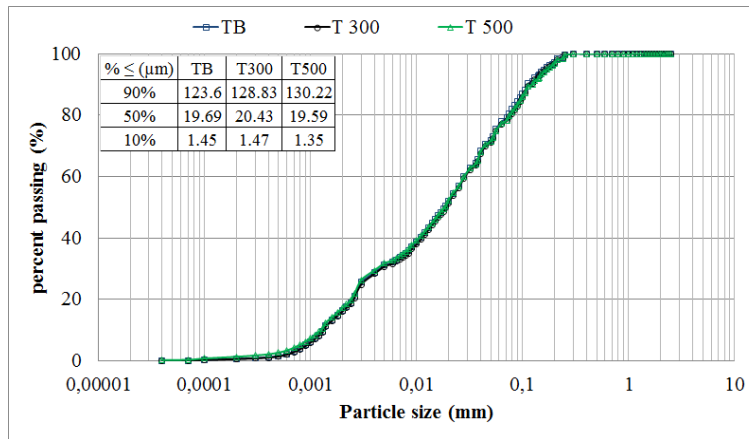
In order to improve the impact of the mechanical activation, which aims to increase the fineness of the material by grinding, the following research intends to grind the tuff separately or by co-grinding with granulate blast furnace slag (GGBFS), as well as co-grinding with Portland cement. The device used to reach this objective was a vibratory disc mill RS 200.

3. Analysis of treated tuff powders

3.1. Calcined tuff

The raw mordenite-rich tuff powder (TB) had a density of 2.29 kg/m³ and a specific surface area of 460 m²/kg. T300 and T500 were assigned to the tuffs after calcination at 300 °C and 500 °C, respectively. The T300 had a lower density (2.254 kg/m³) and a higher specific surface area, 541 m²/kg, compared to TB particles. On the other hand, the reduction in surface area of T500 was coupled with a decrease in density (337 m²/kg and 1.945 kg/m³). Calcination results in an agglomeration of particles up until temperatures of 800 °C, when sintering of the zeolite particles occurs [22–24]. The decrease in the specific surface area of zeolites after calcination is due to a decrease in the microporosity on the crystal surfaces of zeolites, which is caused by slight crystal structure decompositions [15,25].

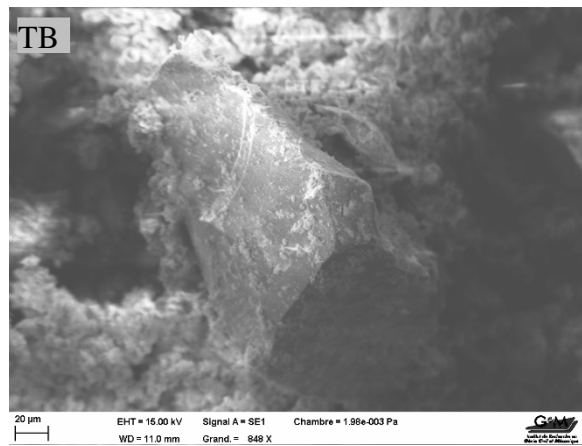
The particle size curves and the SEM micrographs of the two tuffs compared to that of the TB are shown in Fig.1 and Fig. 2, respectively.



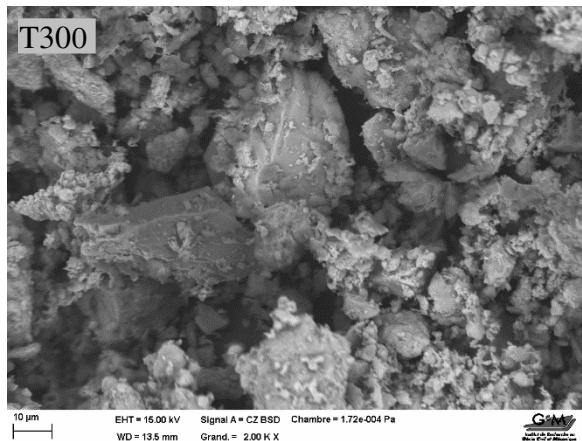
122
123
124
125
126

Fig. Erreur ! Il n'y a pas de texte répondant à ce style dans ce document.1. Particle size distribution curves of T300 and T500 powders

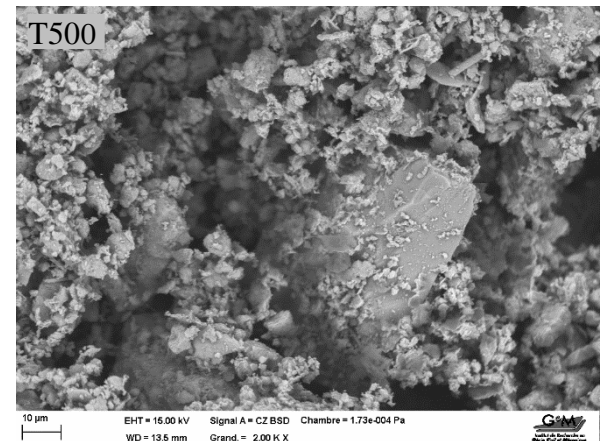
127
128
129
130



131
132
133
134
135
136
137



138
139
140
141
142
143
144
145
146
147
148
149
150



151
152
153
154
155
156
157

Fig. 2. SEM micrograph of the raw and calcined tuff

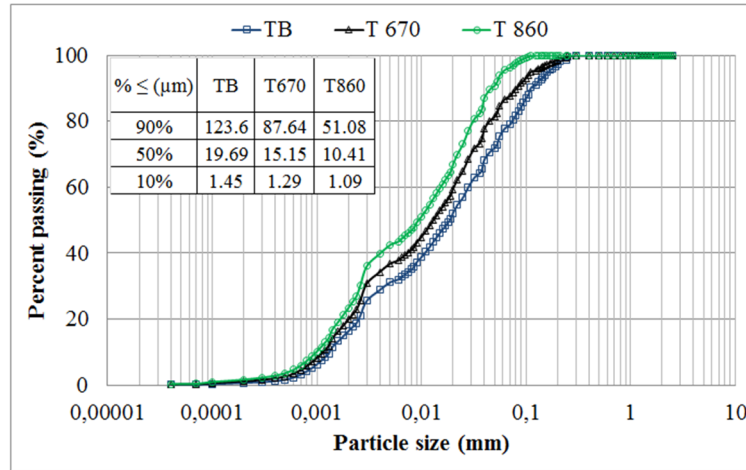
Fig. 1 illustrates that calcination has been associated with a slight increase in the particle size, which is probably due to the agglomeration of particles by sintering at high temperatures [23,26,27]. This effect is qualitatively confirmed in the SEM images shown in Fig. 2. From the images in Fig. 2, it is demonstrated that calcination resulted in an agglomeration of particles, with many of the finer particles becoming adhered to the surfaces of larger particles.

158 3.2. Grinded tuff

159 3.2.1. Grinding to high specific surface area

160 The raw mordenite-rich tuff (TB) powder with a density of 2.29 kg/m³ and a specific surface
161 area of 460 m²/kg was subjected to fine grinding for 14 min and 18 min to reach a specific
162 surface area of 670 and 860 m²/kg, respectively. It is noticed that the density is not affected by
163 the grinding operation.

164 The size and shape of the ground tuffs (T670 and T860) were measured by laser scattering
165 and scanning electron microscopy (SEM) respectively, and results are shown in Fig. 3 and Fig. 4.
166



167
168
169 **Fig. 3.** Particle size distribution curves of T670 and T860 powders
170

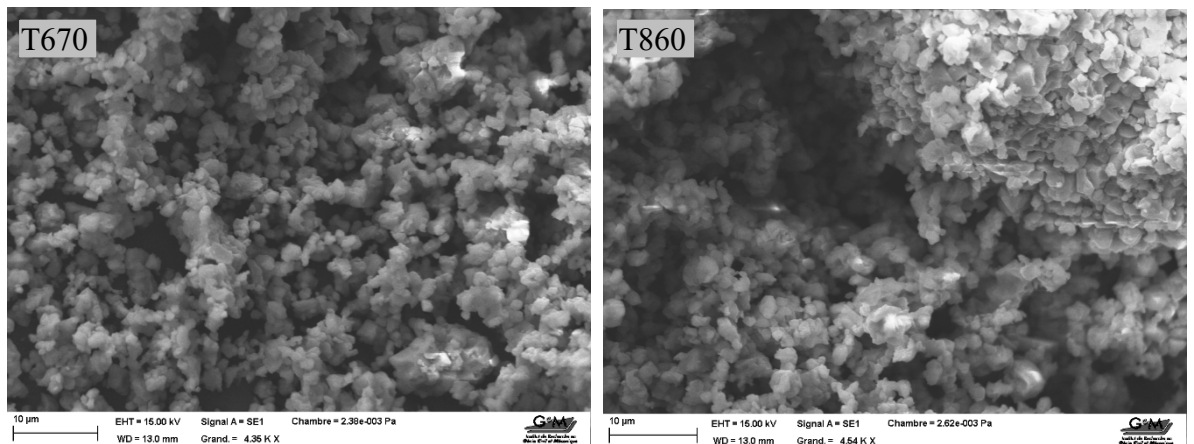


Fig. 4. SEM micrograph of T670 and T860

186 The particle size gradually decreases as the specific surface area increases. The prolonged
187 grinding operation completely eliminated fractions greater than 100 μm and increased the
188 percentage of the fine fractions.

189
190 The SEM micrographs in Fig. 4 indicate that the particles of the tuff after prolonged grinding to
191 high specific surface areas are less agglomerated than in the raw tuff (TB). After grinding, the
192 irregular shape of the particles is transformed into spherical and elliptical ones.

193
194 3.2.2. Grinding with GGBFS

195 The raw mordenite-rich tuff powder (TB) was replaced by 30% (by mass of TB) of GGBFS and
196 underwent two types of grinding. This level was achieved by preliminary tests on the degree of
197 pozzolanicity of the mixture by measuring the amount of free Portlandite in the mixtures.

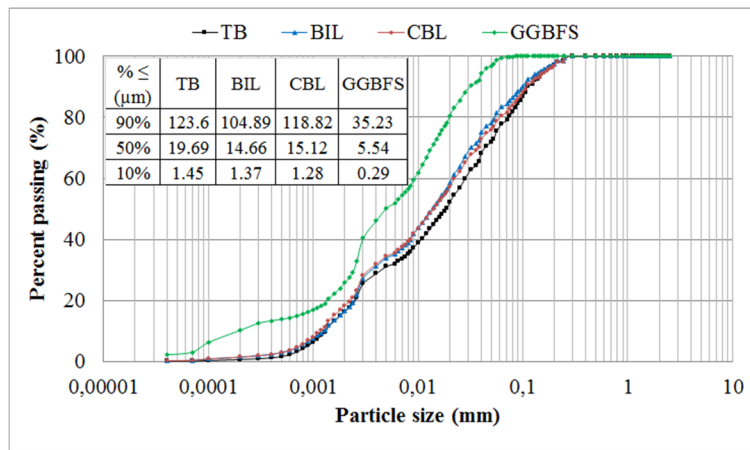
198 *Separate grinding (BIL)*

199 The tuff received in bulk form was crushed and then grounded for 4 min until a specific surface area of 460 m²/kg was obtained, with a density of 2.29 kg/m³. GGBFS with a density of 2.88
 200 kg/m³ and a specific surface area of 405 m²/kg was then mixed with the grounded tuff. After
 201 homogenisation, the powder thus obtained, named BIL, had a density of 2.47 kg/m³ and a
 202 specific surface area of 444 m²/kg.
 203
 204
 205

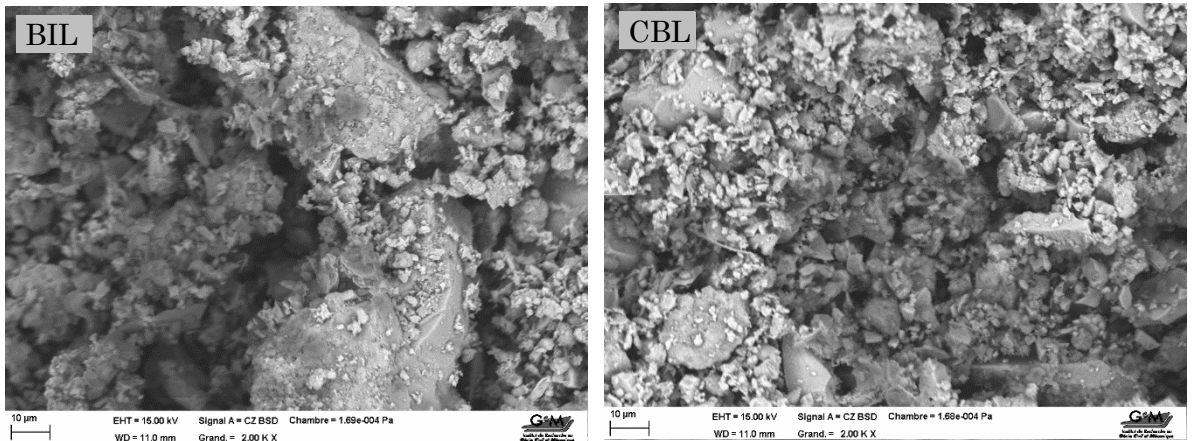
206 *Co-grinding with GGBFS (CBL)*

207 The tuff received in bulk form was crushed and then co-grinded with GGBFS for 3 min to reach
 208 a specific surface area of 434 m²/kg. The density of the powder obtained was 2.51 kg/m³.

209 The size and shape of the BIL and CBL are shown in Fig. 5 and Fig. 6, respectively.
 210



211
 212 **Fig. 5.** Particle size distribution curves of BIL and CBL
 213



214
 215
 216
 217
 218
 219
 220
 221
 222
 223
 224
 225
 226
 227 **Fig. 6.** SEM micrographs of BIL and CBL
 228

229 The SEM micrographs indicate that the BIL and CBL particles have an irregular shape.
 230 From the particle size distribution shown in Fig. 5, it can be seen that the incorporation of
 231 GGBFS into the initial tuff powder reduces the amount of coarse particles. In fact, 90% of them
 232 are less than 104.89 μm and 118.82 μm in the BIL and CBL powders, respectively.
 233
 234

235 *3.2.3. Co-grinding with Portland cement (CBC)*

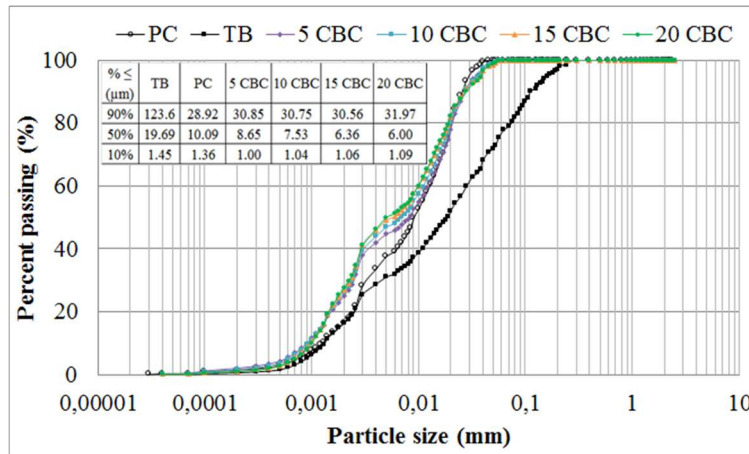
236 The cement CEMI 52.5/R was partially replaced by 5, 10, 15, and 20% of crushed mordenite-
 237 rich tuff (TB) and then grinded for 20min, 18min, 18min, and 15min, respectively to reach a
 238 specific surface area of around 600 m²/kg. The densities and specific surface areas of the

239 powders (cement+% tuff) thus obtained are listed in Table 1. The particle size distribution of tuff
 240 co-grinded with cement is shown in Fig. 7. The SEM morphologies are represented in Fig. 8.
 241 **Table** Erreur ! Il n'y a pas de texte répondant à ce style dans ce document.1: densities and specific surface
 242 areas of tuff co-grinded with Portland cement

| Material | PC | TB | 5 CBC | 10 CBC | 15 CBC | 20 CBC |
|--|------|------|-------|--------|--------|--------|
| Density | 3.14 | 2.29 | 3.04 | 3.02 | 2.87 | 2.79 |
| Specific surface area (m ² /kg) | 440 | 460 | 663 | 613 | 634 | 632 |

243

244



245

246

247

248

249

Fig. Erreur ! Il n'y a pas de texte répondant à ce style dans ce document.7. Particle size distribution curves of tuff co-grinded with Portland cement

250

251

252

253

254

255

256

257

258

259

260

261

262

263

264

265

266

267

268

269

270

271

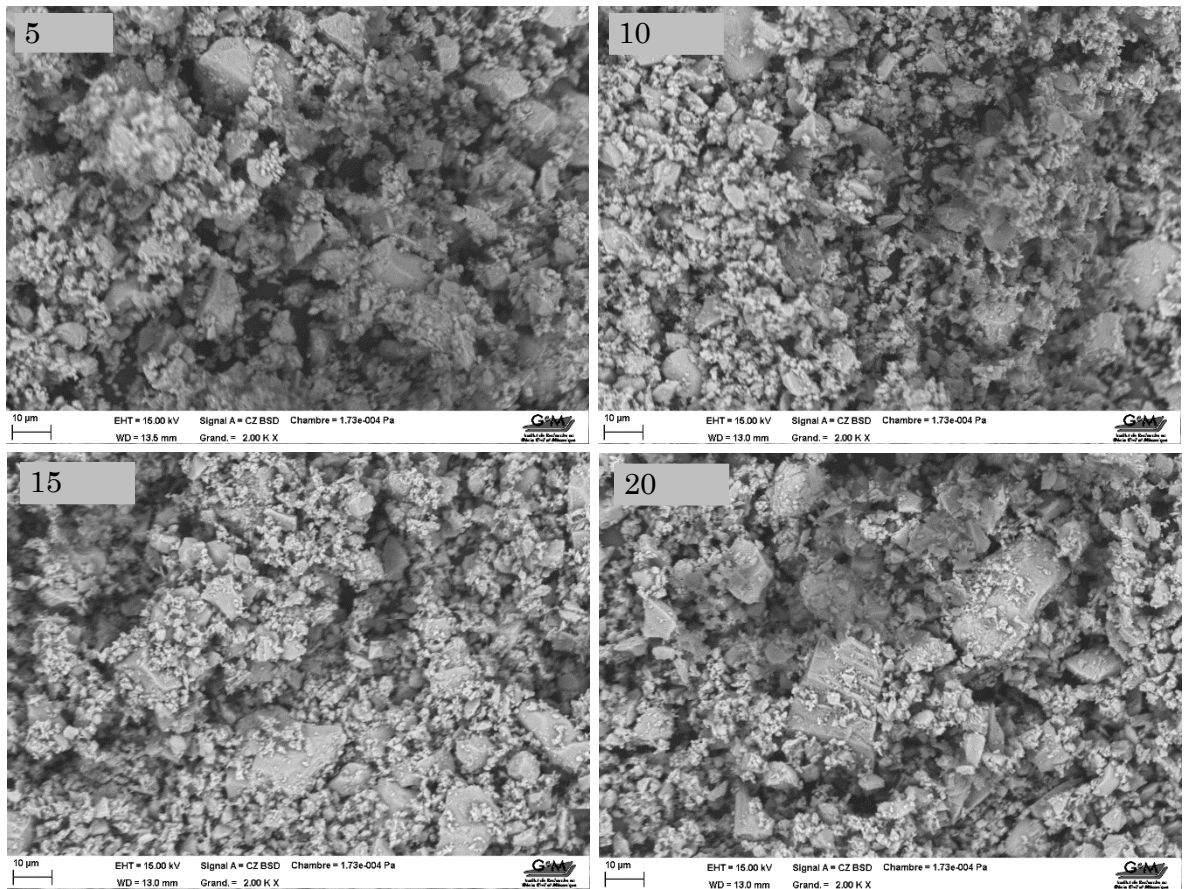


Fig. 8. SEM micrographs of tuff co-grinded with Portland cement

272
 273 From the particle size distribution shown in Fig.7, it can be seen that the mean diameter of the
 274 particles decreases as the amount of tuff co-grinded with Portland cement increases. The cements
 275 resulting from the co-grinding of tuff with cement are slightly finer than Portland cement CEM I
 276 52.5 (PC).

277
 278 Fig. 8 shows that the particles of the powders containing different levels of tuff co-grinded with
 279 PC had an irregular shape. Moreover, other angular-shaped particles with a rough surface texture
 280 relating to PC grains are also observed [28].

281 282 **4. Formulation of cement pastes, cure condition and test methods**

283 To formulate the cement pastes, five substitution rates (by mass) of PC by tuff have been
 284 adopted, including 0, 5, 10, 15, and 20%. Except for GGBFS-incorporating tuff, only one
 285 substitution rate has been studied: 10% of cement was replaced with GGBFS (paste 10L) or
 286 GGBFS-incorporating tuff (pastes BIL and CBL). 24 cement pastes with a water/binder ratio
 287 (w/b) of 0.35 are prepared and mixed according to NF EN 196-1 [29]. The sample curing
 288 conditions have been described in previous research [12].

289 The test methods aim to study the influence of the substitution rate and the method of activation
 290 of the mordenite-rich tuff on the performance of the cement paste. The experimental campaign
 291 includes the normal consistency water requirement, the setting time, monitoring the evolution of
 292 the hydration process (heat and kinetics of hydration), the free Ca(OH)_2 content, the non-
 293 evaporable water and the degree of hydration. The experimental procedure used is that adopted
 294 in [12].

295 **5. Results and discussions**

296 *5.1. Water demand and setting time*

297 The physical properties of fresh cement pastes are listed in Table 2.

298 **Table 2:** physical properties of fresh cement pastes

| Pastes | Water demand (%m/m) | Initial setting time (min) | Final setting time (min) |
|---------|---------------------|----------------------------|--------------------------|
| 100 PC | 30.5 | 59 | 414 |
| 5 TB | 32 | 63 | 359 |
| 10 TB | 32.5 | 65 | 339 |
| 15 TB | 34 | 65 | 305 |
| 20 TB | 35 | 72 | 279 |
| 5 T300 | 32.5 | 67 | 278 |
| 10 T300 | 33.5 | 78 | 274 |
| 15 T300 | 34.0 | 79 | 274 |
| 20 T300 | 35.5 | 91 | 271 |
| 5 T500 | 32.0 | 66 | 279 |
| 10 T500 | 33.0 | 68 | 294 |
| 15 T500 | 33.5 | 74 | 294 |
| 20 T500 | 35.0 | 90 | 339 |
| 5 T670 | 33.0 | 74 | 258 |
| 10 T670 | 34.5 | 90 | 269 |
| 15 T670 | 36.0 | 86 | 327 |
| 20 T670 | 37.5 | 90 | 331 |
| 5 T860 | 33.0 | 64 | 240 |
| 10 T860 | 34.0 | 63 | 254 |

| | | | |
|---------|------|----|-----|
| 15 T860 | 35.5 | 72 | 309 |
| 20 T860 | 36.0 | 74 | 321 |
| 5 CBC | 32.0 | 46 | 309 |
| 10 CBC | 33.5 | 60 | 330 |
| 15 CBC | 35.0 | 58 | 330 |
| 20 CBC | 36.0 | 75 | 363 |
| BIL | 32.0 | 59 | 294 |
| CBL | 31.0 | 55 | 319 |
| 10L | 30.5 | 56 | 339 |

299

300 *Water demand*

301 It can be seen from Table 2 that the tuff treatment techniques cause an increase in the required
302 water percentage proportional to the tuff admixing ratio.

303 The increase in the water demand may be due to the reduction of the base binder (cement) in the
304 mixture as the tuff content increases. Increasing the overall volume of the binder as the tuff
305 content increases requires more water to form a paste of the same standard consistency as the
306 control paste (100 PC) [5].

307 Calcination of the raw tuff (TB) at 300 °C affected slightly the workability of the mixture; in
308 which the water requirement is only increased by less than 3% compared to mixtures containing
309 the untreated tuff. Calcination at 500 °C had no effect on water demand compared to that
310 required in TB pastes. The decrease in water requirement after calcination at 500 °C could be
311 associated with the decrease in specific surface area of T500 compared to T300 [30]. As reported
312 in the literature, calcination of natural zeolites was shown to improve the workability of their
313 pastes through destabilization of the zeolite crystalline structure. In addition, agglomeration of
314 the zeolite particles and the dehydroxylation of the clay impurities during calcination, might also
315 have contributed to the improvement of the workability of the natural zeolite mixtures [15].

316 The specific surface area of T500 decreased by 26.74% compared to that of TB. However, the
317 specific surface of T300 increased by 17.61%. These results demonstrate that calcination at 500
318 °C can reduce the water requirements of the tuff and eliminate the unwanted high water demand.
319 A similar result is reported by previous research [17], which observed that the calcination of a
320 zeolite at different temperatures can reduce or keep the water requirement constant.

321 When heated, pozzolans undergo chemical and structural changes that exhibit two antagonistic
322 effects. The positive effects cover the loss of water in the glassy or zeolite phases and the
323 destruction of the crystal structure. While the negative effect is evidenced by the decrease in
324 specific surface area, devitrification and crystallization [31].

325 Mixtures containing different levels of T670 and T860 show a fairly high water demand, which
326 increases with increasing the content of tuff in the mixtures. This increase is around 7% and 6%
327 in 20 T670 and 20 T860, respectively. The high specific surface area and the porous structure of
328 the zeolite increase the water demand in proportion to the dosage of the zeolite [8,32].

329 Although there is no linear or direct relationship between the specific surface area and the water
330 requirement of tuff, the specific surface area can be referred to as a major parameter explaining
331 the effect of grinding on water requirement. Moreover, although the specific surface area of tuff
332 co-grinded with Portland cement exceeds 600 m²/kg; the need for water increased only slightly
333 (< 3%).

334 Unlike the other blends, those of BIL, CBL, and 10L showed a decrease of 1.54%, 4.62%, and
335 6.15% in water demand of 10 TB, respectively. Adding GGBFS to the tuff increased the
336 fictitious ratio of w/b (visual implication). This is the dilution effect of the mixture. Mixtures
337 containing GGBFS are generally more workable and much easier to set up [33].

338

339 *Setting time*

340 In general, as the replacement levels of the tuff increased, there was a greater delay in setting
341 times. The replacement of the cement at a level of 20% resulted in the greatest delay in the initial
342 setting time, which reached 15 min in the case of the T860 and CBC pastes and 30 min in the
343 case of the T300, T500, and T670 pastes.

344 Whereas the final setting time is prolonged and tends to converge towards that of the control
345 paste as the tuff content increases. In fact, a 20% mass replacement of Portland cement with tuff
346 resulted in an acceleration of the final setting time by 51 min, 75 min, 83 min, 94 min, and 143
347 min in the case of CBC, T500, T670, T860, and T300 pastes, respectively.

348 In comparison with the TB pastes, calcination induces an extension of the initial setting time of
349 about 19 min at a 20% mass replacement of Portland cement. Grinding to a specific surface area
350 of 670 m²/kg has also delayed the initial setting by 25 min, whereas the effect of grinding to a
351 specific surface area of 860 m²/kg was not significant.

352 Compared to the control cement paste and 10TB paste, the inclusion of GGBFS did not show a
353 significant effect in the initial setting but accelerated the final setting. Furthermore, when the
354 level of replacing cement by GGBFS was only 10% and no superplasticizers were incorporated
355 in the paste formulation, the hydration was not retarded. The adsorption of superplasticizers over
356 the surface of cement particles and the lower cement content (dilution effect) can retard the
357 coagulation establishing contacts between particles and the formation of hydrates [34].

358 The final setting times of the pastes resulting from the different activation techniques are
359 significantly less than that of the control paste.

360 In comparison with TB pastes, the replacement of Portland cement by 5 to 15% of calcined tuff
361 significantly accelerates the final setting time. When the tuff was calcined at 300 °C, the final
362 setting time was accelerated by 81 min, 65 min, and 31 min compared to 5 TB, 10 TB, and 15
363 TB, respectively. Calcination at 500 °C accelerated the final setting time by 80 min, 45 min, and
364 11 min, respectively, when compared to 5 TB, 10 TB, and 15 TB. However, the 20 T500 paste
365 prolonged the final setting by 60 min compared to 20 TB.

366 Due to the decrease in the specific surface area of the tuff after calcination at 500 °C, the
367 diffusion of water becomes slower, which leads to a slowing down of the reaction of C₃A, and
368 consequently the rate of crystallization of CSH is slowed down and the setting time is extended
369 [35].

370 Prolonged grinding of the tuff had two opposite effects on the final setting. These effects are
371 related to the tuff content in the pastes. Indeed, the pastes containing 5 and 10% of grinded tuff
372 showed a shorter final setting time than those of TB pastes. The fastest final setting was shown
373 in the cases of 5 T860 and 10 T860 by 119 min, and 85 min, respectively, whereas 15 and 20%
374 content delayed this time.

375 The slowest final setting was observed in the 15 T670 and 20 T670 pastes, which occurred 22
376 min and 52 min after that of 15 TB and 20 TB, respectively.

377 Co-grinding the tuff with Portland cement accelerated the final setting when the content of the
378 tuff was less than 15%. The faster final setting was shown in the case of the 5 CBC paste, which
379 was observed 50 min prior to the 5 TB paste. While in the case of 15 CBC and 20 CBC pastes,
380 this time was delayed by 25 min and 84 min, respectively.

381 The results showed that fine binders (T670, T860 and CBC) had a shorter initial and/or final
382 setting time for 5% and 10% tuff content regardless of the grinding method (co-grinding or
383 separate grinding). Similar results related to the setting time of fine mixtures have been reported
384 by previous researchers [32,36].

385 The standard specifications of EN 197-1 limits the initial setting time to a minimum of 45 min.
386 As seen from Table 2, all cement pastes meet these requirements [37].

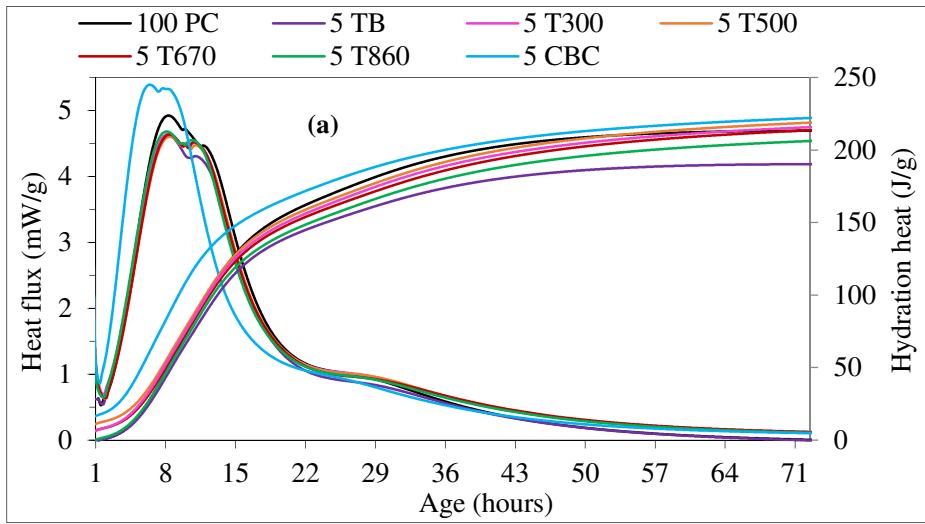
387

388 *4.2. Monitoring the hydration process by isothermal microcalorimetry*

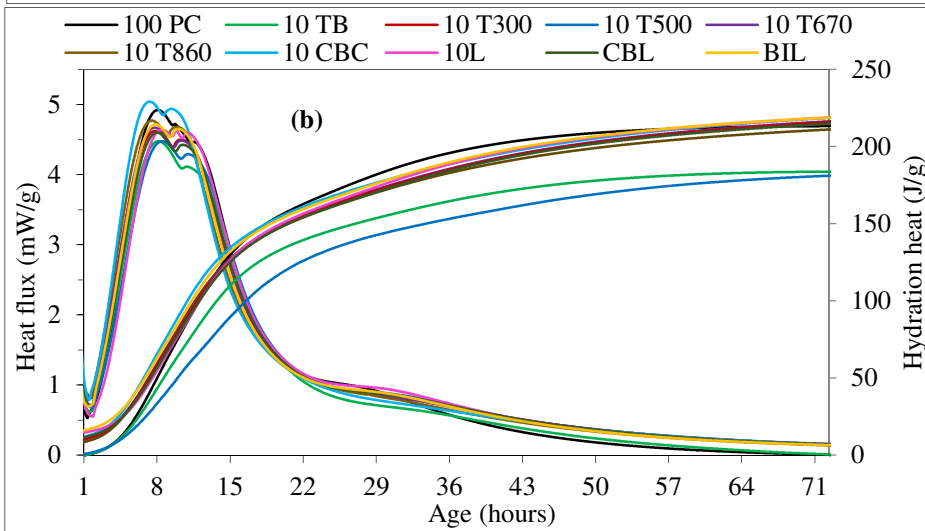
389 Fig. 9 (a-d) shows the rate of heat generation and total heat released as a result of cement
390 hydration obtained from an isothermal calorimetry test at 20 °C.

391

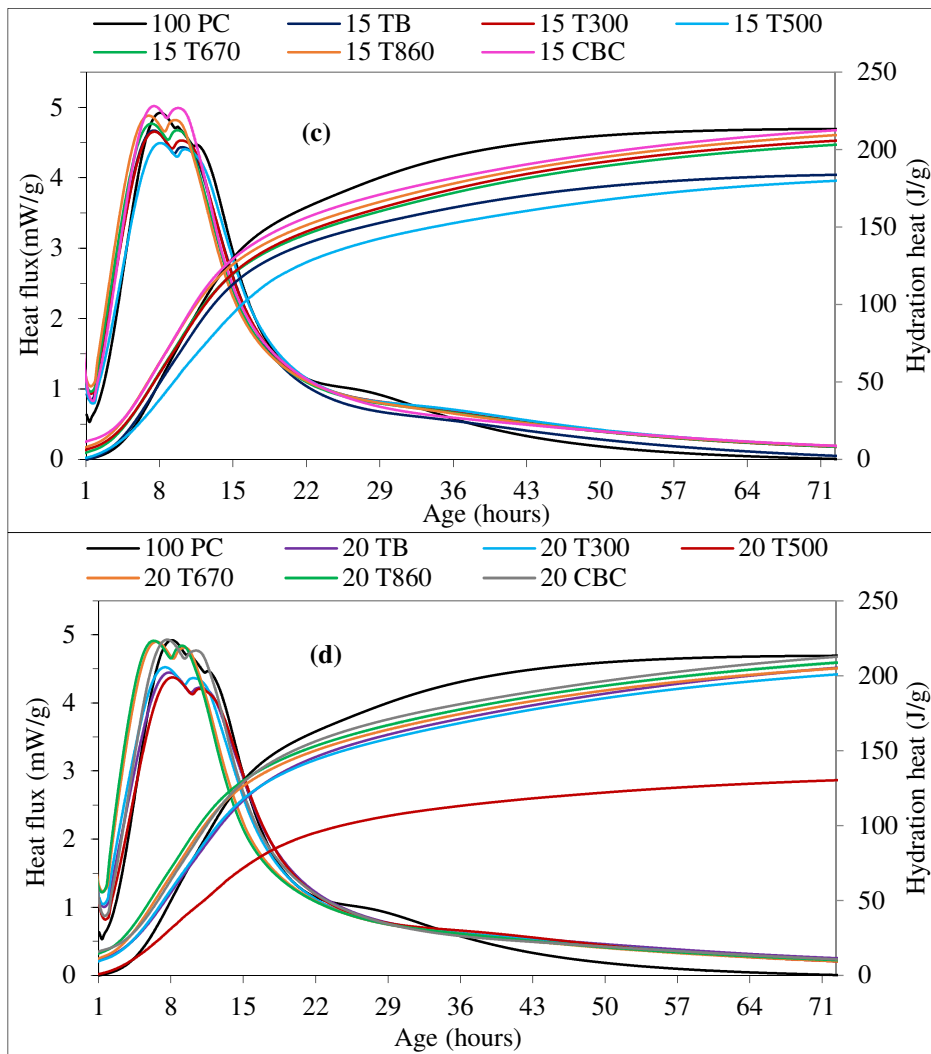
392



393



394



395

396

397

398

Fig. Erreur ! Il n'y a pas de texte répondant à ce style dans ce document.9. Heat flux and hydration heat of the pastes containing the treated tuffs

399

By performing an overarching analysis of the rate of heat generation curves, it can be seen that, except for the pastes containing the T670 and T860 tuff, the intensity of the maximum peak decreases as the content of treated tuff increases. Overall, the tuff may have hindered the total extent of cement hydration [13].

403

Generally, the pastes containing pozzolans have reduced the heat of hydration compared to Portland cement during the first hours of the test [38,39]. Replacing cement with zeolite results in less heat of hydration without a significant reduction in setting time [8].

406

The baseline of heat evolution during the induction period increased as the tuff content increased. Therefore, the development of hydration heat is faster in the initial hydration phase. The addition of the tuff advances the onset of the acceleration period and greatly accelerates the C_3S hydration rate at early stages [40].

410

All treated tuff pastes show a shortened deceleration period and an onset time of the heat flux peak corresponding to the transformation of trisulfoaluminate to monosulfate. This further highlights the accelerating effect of the hydration process by the tuff treated by the different techniques [41].

414

At 72 h, the heat flux of the pastes containing the treated tuff is much greater than that of 100% PC, in particular for the substitution rates of 15% and 20%. This highlights the fact that the activation techniques fully incorporated the tuff in the cement hydration reaction [13].

417

418 A more detailed assessment of the effect of tuff treatment on the hydration of blended systems is
 419 shown in Table 3. This table shows the overall experimental heat of hydration released over a
 420 period of 72 hours (exper hydr heat) and the hydration heat calculated for pure cement (calc hydr
 421 heat). The calculated heat of hydration was calculated according to the following expression:

$$422 \quad Q_{\text{calc hydr heat}} = \frac{Q_{\text{exper hydr heat}}}{100 - \% \text{ substitution}} \times 100 \quad (1)$$

423

424 **Table 3:** Characteristics of the heat flux peak (q_{max}) and the total hydration heat of the different pastes
 425

| Pastes | Intensity of hydration peak (mW/g) | Age of hydration peak (h) | Experimental hydration heat at 72h (J/g) | Calculated hydration heat at 72h (J/g) |
|---------|------------------------------------|---------------------------|--|--|
| 100PC | 4.92 | 7.76 | 213.39 | 213.39 |
| 5 TB | 4.62 | 7.75 | 190.25 | 200.26 |
| 10 TB | 4.62 | 7.75 | 182.62 | 202.91 |
| 15 TB | 4.67 | 7.14 | 183.76 | 216.19 |
| 20 TB | 4.64 | 6.88 | 182.33 | 227.91 |
| 5 T300 | 4.64 | 7.74 | 215.87 | 227.23 |
| 10 T300 | 4.62 | 7.47 | 216.00 | 240.00 |
| 15 T300 | 4.65 | 7.21 | 205.77 | 242.08 |
| 20 T300 | 4.53 | 7.13 | 200.91 | 251.14 |
| 5 T500 | 4.62 | 7.75 | 190.25 | 200.26 |
| 10 T500 | 4.62 | 7.73 | 183.87 | 204.30 |
| 15 T500 | 4.62 | 7.73 | 183.76 | 216.19 |
| 20 T500 | 4.62 | 7.73 | 133.02 | 166.28 |
| 5 T670 | 4.64 | 7.88 | 213.74 | 224.99 |
| 10 T670 | 4.67 | 7.47 | 216.50 | 240.56 |
| 15 T670 | 4.77 | 6.92 | 203.15 | 239.00 |
| 20 T670 | 4.90 | 6.26 | 204.98 | 256.23 |
| 5 T860 | 4.68 | 7.58 | 206.31 | 217.17 |
| 10 T860 | 4.77 | 7.18 | 211.18 | 234.64 |
| 15 T860 | 4.88 | 6.67 | 209.38 | 246.33 |
| 20 T860 | 4.92 | 6.01 | 208.77 | 260.96 |
| 5 CBC | 5.39 | 5.90 | 222.16 | 233.85 |
| 10 CBC | 5.04 | 6.99 | 218.73 | 243.03 |
| 15 CBC | 5.02 | 7.18 | 212.51 | 250.01 |
| 20 CBC | 4.93 | 7.32 | 212.68 | 265.85 |
| BIL | 4.72 | 7.55 | 218.90 | 243.22 |
| CBL | 4.60 | 7.69 | 214.96 | 238.84 |
| 10L | 4.64 | 8.17 | 218.90 | 243.22 |

426 *Calcination: T300 and T500*

427 The intensity of the maximum rate of heat, its time of occurrence, the final heat released and the
428 calculated heat for the T300 and T500 pastes shown in Table 3 are much lower than those
429 measured for the control paste. In addition, the values recorded are higher in the T300 pastes
430 than in the T500 pastes, which align with those of TB pastes.

431 Mixtures incorporating calcined pozzolan exhibit a slight reduction in the induction period and
432 show a higher heat of hydration during this period as compared to the control system [42].

433 The cumulative heat of hydration at 72 hours in the T300 pastes exceeds that of the TB pastes,
434 which surpasses that of the T500 pastes. This implies that calcination at 300 °C makes the tuff
435 more reactive and more mobilizable in hydration reactions than calcination at 500 °C. This may
436 be related to the higher specific surface area of T300 tuff, even though the literature does not
437 observe any direct or generalized correlation between specific surface area and reactivity [43].

438 It should be noted that the 20 T500 paste exhibits both the lowest intense heat flux peak and the
439 lowest experimental and calculated heat of hydration, which are 133.02 J/g and 166.28 J/g,
440 respectively.

441

442 *Prolonged grinding: T670 and T860*

443 The intensity of the maximum rate of heat increases as the content of tuff and its specific surface
444 area increase. Whereas, the start of the acceleration period and the time at which the maximum
445 rate of heat occurs decrease as the tuff content and the specific surface area increase. Grinding
446 the tuff to high specific surface areas dissipates greater heat flux than that of the untreated tuff,
447 but less than Portland cement alone, whereas the time at which the maximum rate of heat occurs
448 is shortened. Finely ground zeolite decreases the induction period time and accelerates the onset
449 of the maximum rate of heat [13,44].

450 The heat of hydration of the T670 and T860 pastes is slightly lower than that of the control
451 pastes but remains significantly higher than that of the TB pastes. As shown in Table 3, the
452 calculated hydration heats of the T670 and T860 pastes are greater than those of the 100 PC and
453 TB pastes, and they increase as the tuff content increases. In general, a pozzolan with a large
454 specific surface area produces a very high heat of hydration [45].

455 The pastes containing prolonged grinding tuff have increased the cumulative heat released after
456 72 h of hydration as compared to the control paste, which proves the tuff's high chemical
457 solubility and the enhancement of the pozzolanic reaction [8].

458

459 *Co-grinding with Portland cement: CBC*

460 The intensity of the maximum rate of heat release decreases as the content of co-grinded tuff
461 with Portland cement increases, while the time required for its onset is delayed.

462 The strong exothermic reactions and the ascending slope of the curves showed that co-grinding
463 the tuff with Portland cement produced a very high heat of hydration that exceeds those of the
464 TB pastes.

465 The heats of hydration of the 5 CBC and 10 CBC pastes are higher as compared to the control
466 paste. Therefore, to prevent thermal shrinkage, the content of tuff co-grinded with Portland
467 cement is limited to no more than 10%.

468

469 *Grinding with GGBFS: BIL, CBL and 10L*

470 As shown in Fig. 9 (b), the BIL paste exhibits a slight acceleration in the C₃S hydration, in which
471 the main exothermic peak of heat flux appears earlier than in CBL, 10 TB, and 100 PC pastes.

472 The addition of GGBFS to the CEM I cement results in a slight acceleration of the hydration of
473 C₃S [46]. However, the GGBFS may have hindered the total extent of cement hydration, shown
474 by the delay of the onset time of the maximum rate of heat and the peak corresponding to the
475 transformation of ettringite into monosulfate in the 10 L paste. This follows the data reported
476 previously by other researchers; the supplementary cementitious materials with low pozzolanic

477 activity decrease the heat of hydration following the cement replacement and the dilution effect
478 [39]. This result is in contrast to that reported by [36], who found that the heat generation rate of
479 mixes incorporating GGBFS is higher than that of pure Portland cement mixture, attributed to
480 the initiation of the pozzolanic reaction.

481 The final heat released and the calculated heat (Table 3) are significantly higher in BIL, CBL and
482 10L pastes than in the 10 TB, and 100 PC pastes. Consequently, thermal shrinkage is to be
483 expected.

484 During hydration, the pastes containing 5% and 10% of tuff co-grinded with Portland cement (5
485 CBC and 10 CBC), as well as pastes incorporating GGBFS (BIL, CBL and 10L), release
486 significantly more heat than control cement paste or those containing untreated tuff. A similar
487 result was found in a cement-grinding test with GGBFS [38]. The dilution effect, expressed by a
488 slight shortening of the setting time of these mixtures, was overcome by the nucleation effect at
489 72 h [36]. This result contradicts the findings of other researchers [20], who found that replacing
490 cement with mineral additions leads to a decrease in the heat of hydration. This phenomenon is
491 directly linked to the dilution effect of mineral additions as well as the fact that pozzolanic
492 reactions release less heat than the hydration of Portland cement.

493

494 *4.3. Free Ca(OH)₂ content*

495 The free Ca(OH)₂ content of hardened pastes prepared with the ordinary Portland cement, as
496 well as pastes prepared with different rates of replacement of PC by untreated or treated tuff was
497 determined by thermogravimetric analysis (TGA) at 7, 28 and 90 days, and the results are shown
498 in Fig. 10 (a-d).

499

500

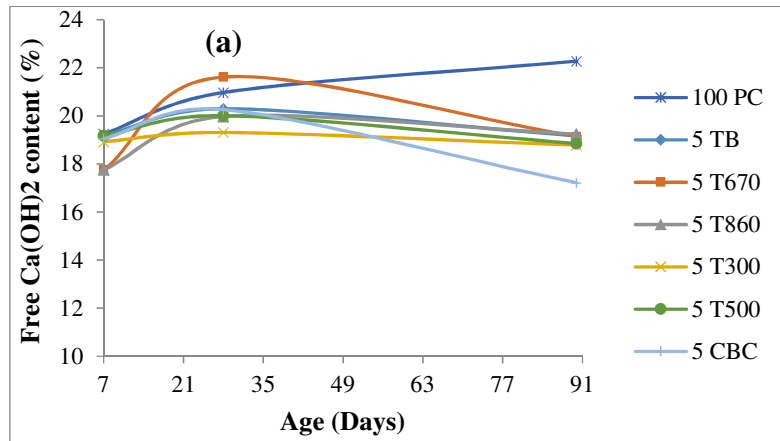
501

502

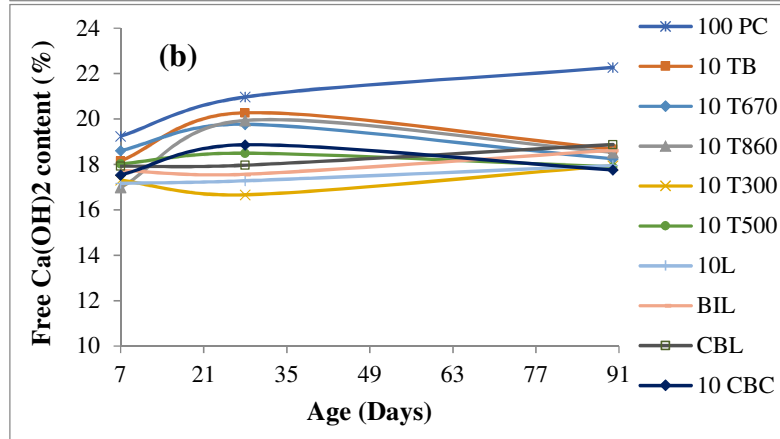
503

504

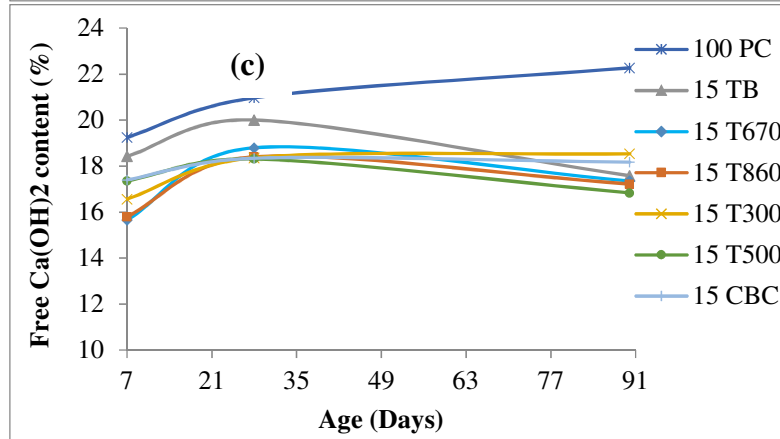
505



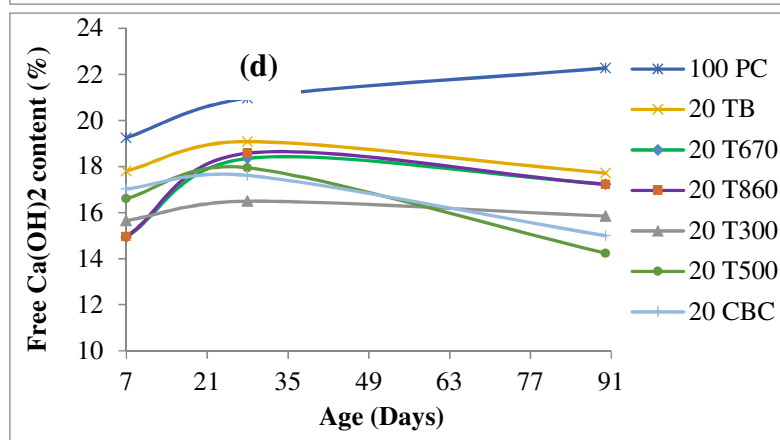
506



507



508



509

510

Fig. 10. free Ca(OH)_2 content of hardened pastes with raw and treated tuff

511 When comparing the hardened pastes containing raw and treated tuff, it was shown that the
512 content of $\text{Ca}(\text{OH})_2$ gradually decreases with the content of activated tuff after 7 days. However,
513 by 28 days, the $\text{Ca}(\text{OH})_2$ content of all the pastes had increased but remained lower than that of
514 100 PC and TB pastes, particularly at the rates of cement replacement by 15% and 20% activated
515 tuff.. Higher $\text{Ca}(\text{OH})_2$ content of the pastes at 28 days can be attributed to an enhanced hydration
516 of Portland cement phase in the blended system [30].

517 At 90 days of age, the free $\text{Ca}(\text{OH})_2$ content of all the pastes containing raw or treated tuff
518 decreased. This outcome is related to the pozzolanic reaction in cement systems [32]. The
519 content of free $\text{Ca}(\text{OH})_2$ significantly decreases when the replacement rate of Portland cement
520 increases, particularly in the 20 T300, 20 T500 and 20 CBC pastes. Overall, calcination at
521 temperatures ranging from 300 °C to 800 °C resulted in little improvements in the pozzolanicity
522 of the zeolites [23].

523
524 The thermal treatment of the tuff at 300 °C confirmed an increase in the pozzolanic activity with
525 respect to the raw tuff as the zeolite (mordenite) destabilised its structure and converted it to a
526 more reactive phase [47]. This outcome is in contrast with the findings of previous research,
527 which reported that calcination of zeolites at temperatures up to 600 °C does not improve
528 pozzolanic reactivity [30]. Other studies have found that thermal treatment of a pozzolan
529 decreases the particle size and the surface area by the aggregation and sintering of the particles,
530 which can result in an insignificant increase or decrease in the pozzolanicity [23,48]. In another
531 study, the authors considered the effect of calcination to be a combination of two opposite
532 effects: an activation depending on the reactivity of the phases and a dis-activation depending on
533 the specific surface area, the decrease in soluble fraction, and the increase in crystallinity [43].
534 According to some researchers, calcination at 400 °C gives the zeolite better reactivity [49], but
535 others reported that thermal treatment at high temperatures (400–1000 °C) is not recommended
536 as pozzolanic activity decreases [30].

537 Increasing the fineness of the tuff regardless of the type of grinding (T670, T860 and CBC) did
538 not have a significant effect on increasing pozzolanic activity. This result is also found in the
539 literature [13,32,36,48]. On the other hand, in a previous study, it was revealed that the
540 mechanically activated pozzolan enhanced the capacity to react with calcium hydroxide to form
541 hydration products [50].

542 Mixtures containing the GGBFS (CBL and BIL) decreased the amount of free $\text{Ca}(\text{OH})_2$ content
543 but did not improve tuff reactivity, while $\text{Ca}(\text{OH})_2$ consumption remained constant compared to
544 the raw tuff.

545 The mixture containing GGBFS alone (10L) consumed more $\text{Ca}(\text{OH})_2$ than the mixtures
546 containing GGBFS mixed with tuff (BIL and CBL) at the same cement substitution rate of
547 10%. This observation confirms that the hydration of GGBFS is gradual and continues for longer
548 periods of time [46,51].

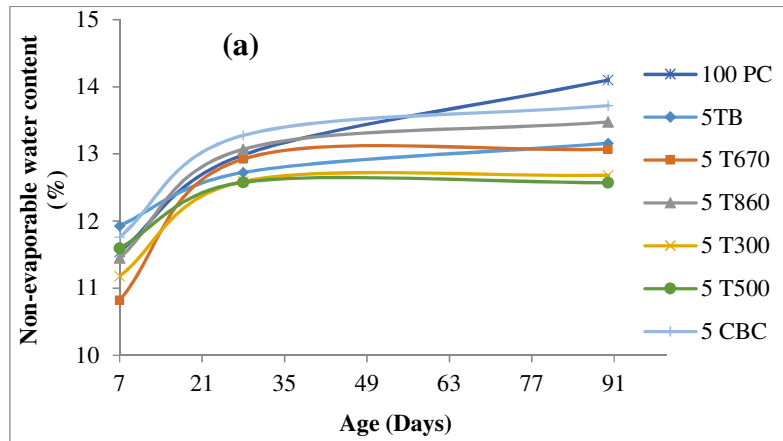
549
550 The improve of workability in mixtures containing GGBFS was beneficial for the hydration
551 reaction of Portland cement and the production of $\text{Ca}(\text{OH})_2$. During this time, the consumption
552 of $\text{Ca}(\text{OH})_2$ in the hydration reaction of GGBFS was less than the additional production of
553 $\text{Ca}(\text{OH})_2$ by the hydration of Portland cement [52].

554 555 *4.4. Non-evaporable water content*

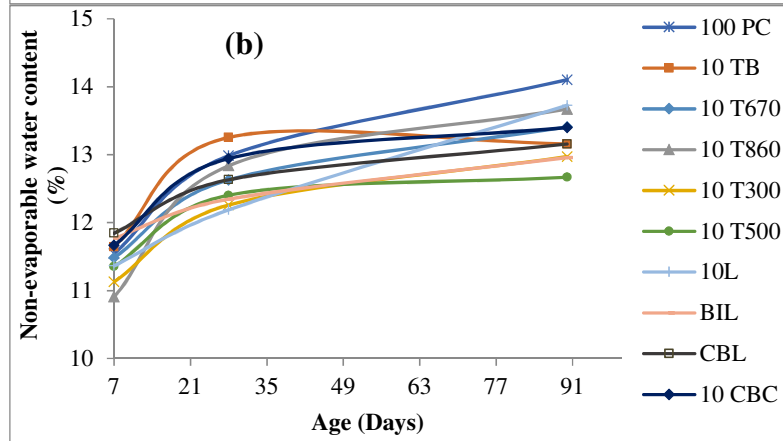
556 The non-evaporable water content of hardened pastes prepared with the ordinary Portland
557 cement as well as the pastes prepared with different rates of replacement of PC by untreated or
558 treated tuff was determined by TGA at 7, 28 and 90 days, and the results are shown in Fig. 11 (a-
559 d).

560

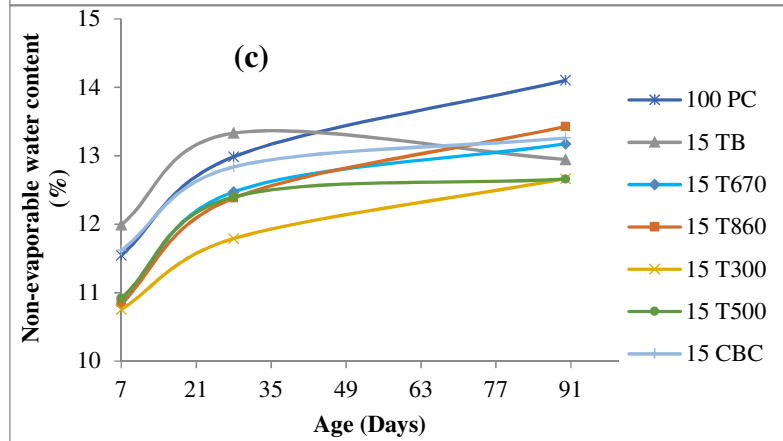
561



562



563



564

565

566

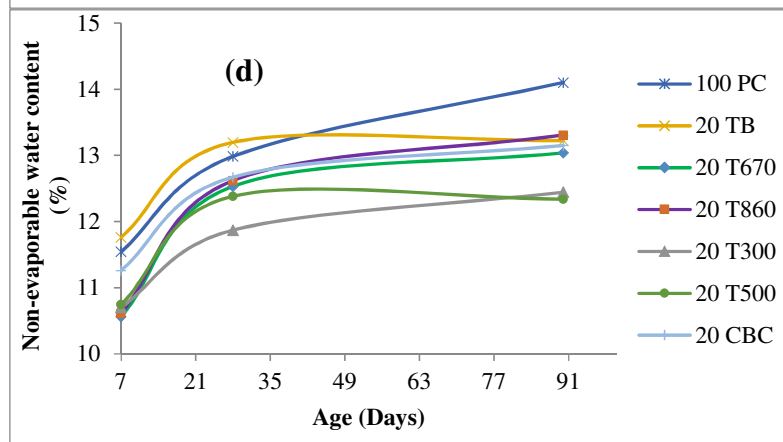


Fig. 11. Non-evaporable water content of hardened pastes with raw and treated tuff

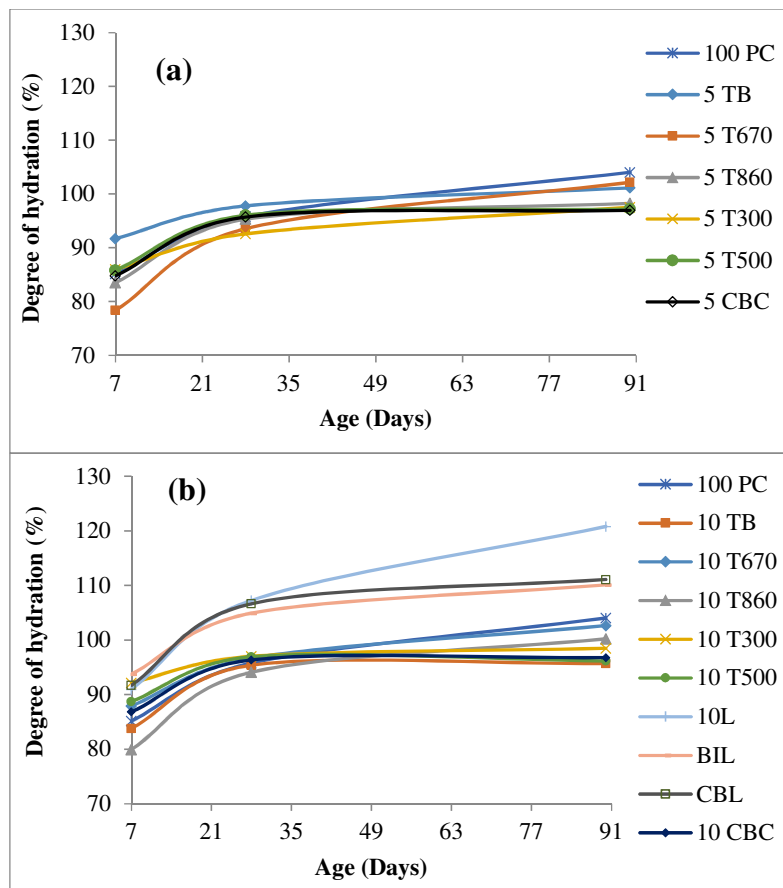
567 Fig. 11 shows that as the curing age increases, so does the amount of non-evaporable water.
 568 Although the hydration reactions are continuous, the kinetic of the non-evaporable water content
 569 over time is relatively low. From 7 to 28 days of age, the non-evaporable water content of the
 570 pastes containing treated tuff has grown significantly but remained lower than that of 100 PC and
 571 TB pastes. At 90 days, the non-evaporable water content continued to increase to exceed,
 572 overall, that of TB pastes but remained lower than that of 100 PC. This usually indicates an
 573 increase in the overall degree of hydration and can indirectly reflect the hydration products in
 574 cementitious systems [46,53,54].

575 Unlike calcination, mechanical activation resulted in a significant increase in non-evaporable
 576 water content. The decrease in the non-evaporable water content may be accompanied by a low
 577 degree of hydration of the blended cements, but in a large part, it is due to the dilution of
 578 Portland cement in the systems [55].

579 While increasing the pozzolan content in cement pastes, the non-evaporable water content
 580 decreases, and the water combined content in hydrates increases. These results are strongly
 581 influenced by the water content of the pastes since the non-evaporable water decreases as the w/b
 582 ratio decreases [56].

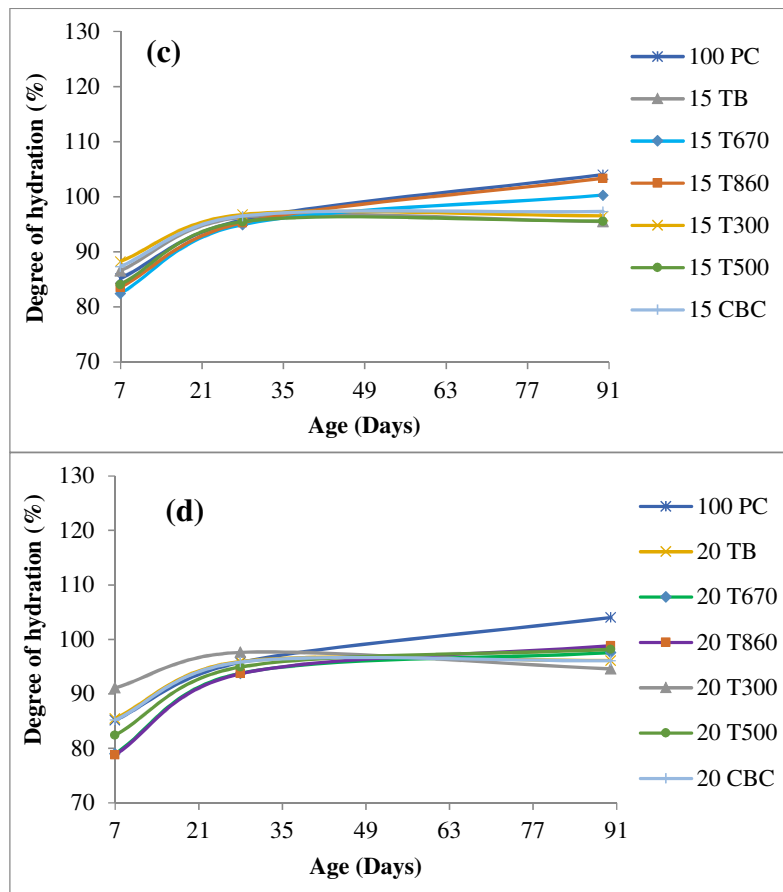
583
 584 *4.5. Degree of hydration*
 585 The degree of hydration of hardened pastes prepared with the ordinary Portland cement as well
 586 as pastes prepared with different rates of replacement of PC by untreated or treated tuff was
 587 determined by TGA at 7, 28 and 90 days, and the results are shown in Fig. 12 (a-d).
 588

589



590

591



592
593
594 **Fig. 12.** Degree of hydration of hardened pastes with raw and treated tuff
595

596 In Fig. 12, the degree of hydration shows a progressive shape over time, but the activation
597 techniques had no significant effect on the raw tuff nor the Portland cement. Mixtures
598 containing GGBFS showed very high degrees of hydration. For cement substitution rates up to
599 15%, calcination at 300 °C slightly increases the degree of hydration, but calcination at 500 °C
600 showed no effect. For cement substitution rates up to 15%, prolonged grinding (T670 and T860)
601 of the tuff appears to increase the degree of hydration. The extents of pozzolanic reaction
602 increases significantly due to the finer grain sizes of the ground pozzolans, while the cement
603 hydration is slightly promoted [57]. The degree of hydration was not improved by co-grinding
604 tuff with cement (CBC) to high specific surface areas. Prolonged grinding of a pozzolan
605 decreases its particle size distribution and increases the rate of dissolution, which accelerates the
606 rate of the pozzolanic reaction and therefore increases the degree of hydration [43].

607 From the figures of non-evaporable water content and degree of hydration, there is no clear
608 correlation nor linear relationship between the two properties. The non-evaporable water content
609 is only an indicator of the degree of hydration since the composition of the hydrates is not
610 precisely known and a certain amount of bound water is lost during the preliminary drying of the
611 samples at 105 °C [31].

612 Non-evaporable water content in hardened pastes is mainly contributed by cement hydration.
613 Only a very small amount of water will be combined by treated or untreated tuff reactions to
614 form non-evaporable water. Therefore, the amount of non-evaporable water can, to a certain
615 extent, represent the cement hydration degree [57]. But, due to the modifications accommodated
616 by the pozzolan in the quantity of the different hydrates as well as in their chemical composition,
617 the determination of the non-evaporable water content is far from sufficient to determine the
618 degree of hydration of the blended cements [58].
619

5. Conclusion

The goal of treatment of the raw mordenite-rich tuff was to improve its physical and compositional properties to allow it to react faster or more completely as pozzolans, resulting in improved performance in cementitious systems. Based on the experimental results, it can be concluded that the treatment techniques improve the performance of the raw mordenite-rich tuff.

The following are the findings that can be drawn:

Calcination resulted in particle agglomeration, with many of the finer particles becoming adhered to the surfaces of larger particles, which slightly increased the particle size of calcined tuff. Grinding reduces the amount of coarse particles, increases the percentage of the fine fractions, and makes them less agglomerated than in the raw state.

As the tuff content increases, more water is required to make a paste with the same standard consistency as the control paste. Thermal treatment and co-grinding with Portland cement appear to have a minor effect on the water requirement, which appears to grow with prolonged grinding to high specific surface areas. Adding GGBFS to the tuff increased the fictitious ratio of w/b. This is the dilution effect of the mixture, which resulted in the mixture being more workable and much easier to set up.

Calcination extends the initial setting, but accelerates the final setting and the hardening of the cement paste. Regardless of grinding procedure, fine binders (T670, T860 and CBC) exhibited shorter initial and/or final setting time for 5% and 10% tuff content. Furthermore, the slowest final setting was found in pastes containing 15% and 20% of prolonged ground tuff. Incorporating GGBFS had no significant effect on the initial setting but accelerated the final setting. Furthermore, even when just 10% of the cement was replaced by GGBFS and no superplasticizers were used in the paste formulation, the hydration was not retarded. The standard specifications of EN 197-1 limit the initial setting time to a minimum of 45 min. All of the cement pastes meet these requirements.

Pre-treatment of the tuff advances the onset of the acceleration period and greatly accelerates the C3S hydration rate at early stages, resulting in faster and greater hydration heat development than 100 PC and TB pastes. Treated tuff pastes show a shortened deceleration period and an onset time of the heat flux peak corresponding to the transformation of trisulfoaluminate to monosulfate. This further highlights the accelerating effect of the treated tuff on the hydration process. After 72 h of cement hydration, the heat flux of the pastes containing treated tuff is much greater than that of 100 PC paste. This demonstrates how activation techniques fully incorporated the treated tuff into the cement hydration reaction.

Thermal treatment of the tuff at 300 °C resulted in an increase in pozzolanic activity compared to raw tuff. Calcination at 500 °C increased the particle size and reduced the specific surface area of the tuff due to particle aggregation and sintering, resulting in a low increase in pozzolanicity. Mechanically activating tuff did not significantly improve its ability to react with calcium hydroxide.

Although the hydration reactions are continuous, the kinetics of the non-evaporable water content over time is relatively low. Unlike calcination, mechanical activation resulted in a significant increase in non-evaporable water content. After 90 days of hydration, pastes incorporating treated tuffs showed non-evaporable water greater than those of TB pastes. This generally indicates an increase in the overall degree of hydration and can indirectly reflect the hydration products in cementitious systems.

Mixtures containing GGBFS showed the highest degrees of hydration. Calcination at 300 °C slightly enhances the degree of hydration, whereas calcination at 500 °C has little effect. Prolonged grinding of the tuff reduces particle size distribution and increases the rate of dissolution, which accelerates the rate of the pozzolanic reaction and therefore increases the degree of hydration, but this case was not shown by co-grinding the tuff with Portland cement.

671 The findings indicate that there is no evident correlation or linear relationship between non-
672 evaporable water content and degree of hydration. Because the composition of the hydrates is not
673 exactly known and a certain amount of bound water is lost during the preliminary drying of the
674 samples at 105 °C, the non-evaporable water content is only an indicator of the degree of
675 hydration.

677 **References**

- 678 [1] B. Ahmadi, M. Shekarchi, Use of natural zeolite as a supplementary cementitious
679 material, *Cem. Concr. Compos.* 32 (2010) 134–141.
680 doi:10.1016/j.cemconcomp.2009.10.006.
- 681 [2] C. Bilim, Properties of cement mortars containing clinoptilolite as a supplementary
682 cementitious material, *Constr. Build. Mater.* 25 (2011) 3175–3180.
683 doi:10.1016/j.conbuildmat.2011.02.006.
- 684 [3] I. Marantos, G. Christidis, M. Ulmanu, Zeolite formation and deposit, in: *Handb. Nat.*
685 *Zeolites*, Bentham Science, Sharjah, United Arab Emirates, 2012.
- 686 [4] K. Stocker, M. Ellersdorfer, M. Lehner, J.G. Raith, Characterization and Utilization of
687 Natural Zeolites in Technical Applications, *Berg- Und Hüttenmännische Monatshefte.* 162
688 (2017) 142–147. doi:10.1007/s00501-017-0596-5.
- 689 [5] D.A. Adesanya, A.A. Raheem, Development of corn cob ash blended cement, *Constr.*
690 *Build. Mater.* 23 (2009) 347–352. doi:10.1016/j.conbuildmat.2007.11.013.
- 691 [6] C. Florez, O. Restrepo-Baena, J. I. Tobon, Effects of calcination and milling pre-
692 treatments on natural zeolites as a supplementary cementitious material, *Constr. Build.*
693 *Mater.* 310 (2021) 125220. doi:https://doi.org/10.1016/j.conbuildmat.2021.125220.
- 694 [7] J.L. Costafreda, D.A. Mart, L. Presa, J. Luis Parra, Effects of a Natural Mordenite as
695 Pozzolan Material in the Evolution of Mortar Settings, *Materials (Basel).* 14 (2021) 5343.
696 doi:https://doi.org/10.3390/ma14185343.
- 697 [8] V. Lilkov, O. Petrov, Y. Tzvetanova, Rheological, porosimetric, and SEM studies of
698 cements with additions of natural zeolites, *Clays Miner.* 46 (2011) 225–232.
699 doi:10.1180/claymin.2011.046.2.225.
- 700 [9] K.P. Kitsopoulos, A.C. Dunham, Heulandite and mordenite-rich tuffs from Greece: a
701 potential source for pozzolanic materials, 583 (1996) 576–583.
- 702 [10] R. Vigil de la Villa, N. Özkan, R. García, E. Villar-cociña, M. Frías, Pozzolan activity
703 and alkaline reactivity of a mordenite-rich tuff, *Microporous Mesoporous Mater.* 126
704 (2009) 125–132. doi:10.1016/j.micromeso.2009.05.029.
- 705 [11] G. Mertens, R. Snellings, K. Van Balen, B. Bicer-simsir, P. Verlooy, J. Elsen, Pozzolan
706 reactions of common natural zeolites with lime and parameters affecting their reactivity,
707 *Cem. Concr. Res.* 39 (2009) 233–240. doi:10.1016/j.cemconres.2008.11.008.
- 708 [12] M. Meziani, N. Leklou, O. Amiri, N. Chelouah, Physical and mechanical studies on
709 binary blended Portland cements containing mordenite-rich tuff and limestone filler,
710 *Matériaux & Techniques.* 303 (2019) 1–12.
- 711 [13] L.E. Burris, M. C G Juenger, Milling as a pretreatment method for increasing the
712 reactivity of natural zeolites for use as supplementary cementitious materials, *Cem. Concr.*
713 *Compos.* 65 (2016) 163–170. doi:10.1016/j.cemconcomp.2015.09.008.
- 714 [14] J.J. Chen, L.G. Li, P.L. Ng, A.K.H. Kwan, Effects of superfine zeolite on strength,
715 flowability and cohesiveness of cementitious paste, *Cem. Concr. Compos.* 83 (2017) 101–
716 110. doi:10.1016/j.cemconcomp.2017.06.010.
- 717 [15] S. Seraj, R.D. Ferron, M.C.G. Juenger, Calcining natural zeolites to improve their effect
718 on cementitious mixture workability, *Cem. Concr. Res.* 85 (2016) 102–110.
719 doi:10.1016/j.cemconres.2016.04.002.
- 720 [16] D. Güngör, S. Ozen, Development and characterization of clinoptilolite-, mordenite-, and
721 analcime-based geopolymers: A comparative study., *Case Stud. Constr. Mater.* 15 (2021)

- 722 e00576. doi:10.1016/j.cscm.2021.e00576.
- 723 [17] A. Askarinejad, F. Zisti, A. Pourkhorshidi, T. Parhizkar, Hydrothermal preparation of
724 natural pozzolan nanostructures as a new route to activate cement replacement materials,
725 *Synth. React. Inorganic, Met. Nano-Metal Chem.* 48 (2016) 1157–1162.
726 doi:10.1080/15533174.2013.776595.
- 727 [18] M. Frías, O. Rodríguez, M.I. Sanchez de Rojas, E. Villar-cociña, M. S. Rodrigues, H.
728 Savastano Junior, Advances on the development of ternary cements elaborated with
729 biomass ashes coming from different activation process, *Constr. Building Mater.* 136
730 (2017) 73–80. doi:10.1016/j.conbuildmat.2017.01.018.
- 731 [19] M. Frías, R. Vigil de la ville, R. García, S. Martínez, E. Villar, I. Vegas, Effect of a high
732 content in activated carbon waste on low clinker cement microstructure and properties,
733 *Constr. Build. Mater.* 184 (2018) 11–19. doi:10.1016/j.conbuildmat.2018.06.216.
- 734 [20] M.H. Cornejo, J. Elsen, C. Paredes, H. Baykara, Thermomechanical treatment of two
735 Ecuadorian zeolite-rich tuffs and their potential usage as supplementary cementitious
736 materials, *J. Therm. Anal. Calorim.* 115 (2014) 309–321. doi:10.1007/s10973-013-3345-
737 3.
- 738 [21] A. Tironi, A.N. Scian, E.F. Irassar, Blended cements with limestone filler and kaolinitic
739 calcined clay: Filler and pozzolanic effects, *J. Mater. Civ. Eng.* 29 (2017) 1–8.
740 doi:10.1061/(ASCE)MT.1943-5533.0001965.
- 741 [22] E. Liebig, E. Althaus, Pozzolanic activity of volcanic tuff and suevite: effects of
742 calcination, *Cem. Concr. Res.* 28 (1998) 567–575.
- 743 [23] L.E. Burris, M.C.G. Juenger, Effect of calcination on the reactivity of natural clinoptilolite
744 zeolites used as supplementary cementitious materials, *Constr. Build. Mater.* 258 (2020)
745 119988. doi:10.1016/j.conbuildmat.2020.119988.
- 746 [24] M. Liu, Y. Zhao, Z. Yu, Effects of sewage sludge ash produced at different calcining
747 temperatures on pore structure and durability of cement mortars, *J. Mater. Cycles Waste*
748 *Manag.* (2021). doi:10.1007/s10163-021-01174-y.
- 749 [25] G.E. Christidis, D. Moraetis, E. Keheyan, L. Akhalbedashvili, N. Kekelidze, R.
750 Gevorkyan, H. Yeritsyan, H. Sargsyan, Chemical and thermal modification of natural
751 HEU -type zeolitic materials from Armenia , Georgia and Greece, *App.* 24 (2003) 79–91.
752 doi:10.1016/S0169-1317(03)00150-9.
- 753 [26] A. Ates, C. Hardacre, The effect of various treatment conditions on natural zeolites : Ion
754 exchange , acidic , thermal and steam treatments, *J. Colloid Interface Sci.* 372 (2012) 130–
755 140. doi:10.1016/j.jcis.2012.01.017.
- 756 [27] K. Elaiopoulos, T. Perraki, E. Grigoropoulou, Monitoring the effect of hydrothermal
757 treatments on the structure of a natural zeolite through a combined XRD, FTIR, XRF,
758 SEM and N₂-porosimetry analysis, *Microporous Mesoporous Mater.* 134 (2010) 29–43.
759 doi:10.1016/j.micromeso.2010.05.004.
- 760 [28] B. Felekoglu, S. Türkel, H. Kalyoncu, Optimization of fineness to maximize the strength
761 activity of high-calcium ground fly ash–Portland cement composites, *Constr. Building*
762 *Mater.* 23 (2009) 2053–2061. doi:10.1016/j.conbuildmat.2008.08.024.
- 763 [29] NF EN 196-1, Methods of testing cement - Part 1 : Determination of strength, european
764 committee for standardization, Bruxelles, 2016.
- 765 [30] E. Küçükyıldırım, B. Uzal, Characteristics of calcined natural zeolites for use in high-
766 performance pozzolan blended cements, *Constr. Build. Mater.* 73 (2014) 229–234.
767 doi:10.1016/j.conbuildmat.2014.09.081.
- 768 [31] F. Massazza, Pozzolana and Pozzolanic Cements, in: P.C. Hewlett (Ed.), *Lea's Chem.*
769 *Cem. Concr.*, Elsevier B, Oxford, 1998: p. 1057.
- 770 [32] E. Ghiasvand, A. Ramezaniapour, A. Ramezaniapour, M. Namian, R. Slami, M.
771 Gharechaei, Effect of grinding method and particle size distribution on early-age
772 properties of blended cements, *Adv. Cem. Res.* 27 (2015) 201–213.

- 773 [33] R. Doug Hooton, Canadian use of ground granulated blast-furnace slag as a
774 supplementary cementing material for enhanced performance of concrete, *Can. J. Civ.*
775 *Eng.* 27 (2000) 754–760.
- 776 [34] J.J. Brooks, M.A. Megat Johari, M. Mazloom, Effect of admixtures on the setting times of
777 high-strength, *Cem. Concr. Compos.* 22 (2000) 293–301.
- 778 [35] B. Yilmaz, N. Ediz, The use of raw and calcined diatomite in cement production, *Cem.*
779 *Concr. Compos.* 30 (2008) 202–211. doi:10.1016/j.cemconcomp.2007.08.003.
- 780 [36] E. Ghiasvand, A.A. Ramezani pour, A.M. Ramezani pour, Effect of grinding method
781 and particle size distribution on the properties of Portland-pozzolan cement, *Constr. Build.*
782 *Mater.* 53 (2014) 547–554. doi:10.1016/j.conbuildmat.2013.11.072.
- 783 [37] NF EN 197-1, Cement — Part 1: Composition, specifications and conformity criteria for
784 common cements, european committee for standardization, Bruxelles, 2001.
- 785 [38] H. Binici, O. Aksogan, I. H. Cagatay, M. Tokyay, E. Emsen, The effect of particle size
786 distribution on the properties of blended cements incorporating GGBFS and natural
787 pozzolan (NP), *Powder Technol.* 177 (2007) 140–147. doi:10.1016/j.powtec.2007.03.033.
- 788 [39] M. Bohác, M. Palou, R. Novotny, J. Masilko, D. Všiansky, T. Stane, Investigation on
789 early hydration of ternary Portland cement-blast-furnace slag – metakaolin blends, *Constr.*
790 *Build. Mater.* 64 (2014) 333–341. doi:10.1016/j.conbuildmat.2014.04.018.
- 791 [40] R. Snellings, G. Mertens, Ö. Cizer, J. Elsen, Early age hydration and pozzolanic reaction
792 in natural zeolite blended cements : Reaction kinetics and products by in situ synchrotron
793 X-ray powder diffraction, *Cem. Concr. Res.* 40 (2010) 1704–1713.
794 doi:10.1016/j.cemconres.2010.08.012.
- 795 [41] M.C.G. Juenger, R. Siddique, Recent advances in understanding the role of supplementary
796 cementitious materials in concrete, *Cem. Concr. Res.* 78 (2015) 71–80.
797 doi:10.1016/j.cemconres.2015.03.018.
- 798 [42] A. Alujas, R. Fernández, R. Quintana, K.L. Scrivener, F. Martirena, Pozzolanic reactivity
799 of low grade kaolinitic clays : Influence of calcination temperature and impact of
800 calcination products on OPC hydration, *Appl. Clay Sci.* 108 (2015) 94–101.
801 doi:10.1016/j.clay.2015.01.028.
- 802 [43] C. Shi, An overview on the activation of reactivity of natural pozzolans, *Can. J. Civ. Eng.*
803 28 (2001) 778–786. doi:10.1139/cjce-28-5-778.
- 804 [44] J. Cheung, A. Jeknavorian, L. Roberts, D. Silva, Impact of admixtures on the hydration
805 kinetics of Portland cement, *Cem. Concr. Res.* 41 (2011) 1289–1309.
806 doi:10.1016/j.cemconres.2011.03.005.
- 807 [45] R. Snellings, G. Mertens, J. Elsen, Calorimetric evolution of the early pozzolanic reaction
808 of natural zeolites, *J. Therm. Anal. Calorim.* 101 (2010) 97–105. doi:10.1007/s10973-009-
809 0449-x.
- 810 [46] O.R. Ogirigbo, L. Black, Influence of slag composition and temperature on the hydration
811 and microstructure of slag blended cements, *Constr. Build. Mater.* 126 (2016) 496–507.
812 doi:10.1016/j.conbuildmat.2016.09.057.
- 813 [47] R. Vigi de la Villa, R. Fernandez, O. Rodriguez, F. Garcia, E. Villar-Cocina, M. Frias,
814 Evolution of the pozzolanic activity of a thermally treated zeolite, *J. Mater. Sci.* 48 (2013)
815 3213–3224. doi:10.1007/s10853-012-7101-z.
- 816 [48] B. Fabbri, S. Gualtieri, C. Leonardi, Modifications induced by the thermal treatment of
817 kaolin and determination of reactivity of metakaolin, *Appl. Clay Sci.* 73 (2013) 2–10.
818 doi:10.1016/j.clay.2012.09.019.
- 819 [49] T. Perraki, G. Kakali, E. Kontori, Characterization and pozzolanic activity of thermally
820 treated zeolite, *J. Therm. Anal. Calorim.* 82 (2005) 109–113.
- 821 [50] G. Yao, T. Cui, Y. Su, C. Anning, J. Wang, X. Lyu, Hydration properties of mechanical
822 activated muscovite in the presence of calcium oxide, *Clays Clay Miner.* (2020).
823 doi:10.1007/s42860-020-00095-5.

- 824 [51] J.I. Esclante, L.Y. Gomez, K.K. Johal, G. Mendoza, H. Mancha, J. Mendez, Reactivity of
825 blast-furnace slag in Portland cement blends hydrated under different conditions, *Cem.*
826 *Concr. Res.* 31 (2001) 1403–1409.
- 827 [52] S. Wan, X. Zhou, M. Zhou, Y. Han, Y. Chen, J. Geng, T. Wang, S. Xu, Z. Qiu, H. Hou,
828 Hydration characteristics and modeling of ternary system of municipal solid wastes
829 incineration fly ash-blast furnace slag-cement, *Constr. Build. Mater.* 180 (2018) 154–166.
830 doi:10.1016/j.conbuildmat.2018.05.277.
- 831 [53] C. Lijuan, G. Liping, C. Bo, C. Yuanzhang, Effects of curing age on compressive and
832 tensile stress-strain behavior of ecological high ductility cementitious composites, *J.*
833 *Southeast Univ.* 36 (2020) 73–80.
- 834 [54] C.C. Castellano, V.L. Bonavetti, H.A. Donza, E.F. Irassar, The effect of w/b and
835 temperature on the hydration and strength of blastfurnace slag cements, *Constr. Build.*
836 *Mater.* 111 (2016) 679–688. doi:10.1016/j.conbuildmat.2015.11.001.
- 837 [55] A. Bougara, C. Lynsdale, N.B. Milestone, The influence of slag properties, mix
838 parameters and curing temperature on hydration and strength development of slag/cement
839 blends, *Constr. Build. Mater.* 187 (2018) 339–347.
840 doi:10.1016/j.conbuildmat.2018.07.166.
- 841 [56] V. Yogendran, B.W. Langan, M.A. Ward, Hydration of cement and silica fume paste,
842 *Cem. Concr. Res.* 21 (1991) 691–708.
- 843 [57] Y. Sun, H. Lee, Research on properties evolution of ultrafine fly ash and cement
844 composite, *Constr. Build. Mater.* 261 (2020) 119935.
845 doi:10.1016/j.conbuildmat.2020.119935.
- 846 [58] M.H. Zhang, O.E. Gjorv, Effect of silica fume on cement hydration in low porosity
847 cement pastes, *Cem. Concr. Res.* 21 (1991) 800–808.